ELSEVIER

Journal of Photochemistry and Photobiology A: Chemistry 130 (2000) 95–100

Journal of Photochemistry and Photobiology A:Chemistry

www.elsevier.nl/locate/jphotochem

Influence of redoxinert counterions on photoinduced intermolecular electron transfer rates in dichloromethane

T. Kluge, H. Knoll *

Wilhelm-Ostwald-Institut für Physikalische und Theoretische Chemie der Universität Leipzig, Linnéstr. 2, D-04103 Leipzig, Germany

Received 9 October 1999; accepted 12 October 1999

Abstract

Rate constants k_q of the fluorescence quenching of 9,10-dicyanoanthracene by bromide and chloride ions and of 9-cyanoanthracene by bromide ions were determined in the low polar solvent dichloromethane with a series of tetra-alkylammonium counterions. Cation size dependent electron transfer rate constants k_{et} were derived from k_q, and were fitted to a nonadiabatic electron transfer model equation. Because of ion pair formation in dichloromethane electrostatic interactions of the redoxinert countercations during electron transfer were considered. Accordingly, the position of the countercation within the precursor complex had to be described.

The electronic coupling matrix element derived by fitting of the experimental data is in satisfactory agreement with results of simple quantum chemical calculations. ©2000 Elsevier Science S.A. All rights reserved.

Keywords: Counterions; Dichloromethane; Intermolecular; Electron transfer

1. Introduction and theory

Recent studies of Piotrowiak et al. show the influence of specific ion pairing effects on intramolecular electron transfer rates [1–3]. Similar effects can be expected in intermolecular electron transfer which were observed in [1] but not studied and discussed in detail. Other authors found that redoxinert countercations may influence rates of anion-anion electron transfer [4,5] and the change of the rate controlling step from one typical inner-sphere and outer-sphere reorganization to one of anion migration [6]. Specific salt effects on the excited-state electron transfer quenching reactions of ruthenium(II)-diimine photosensitizers were studied by Hoffman et al. [7–9]. Marcus discussed ion-pairing mainly with respect to intramolecular electron transfer rates [10]. In a preliminary paper [11] we have shown, that the rate constants k_q of the electron transfer quenching of singlet excited 9, 10-dicyanoanthracene (DCA) and 9-cyanoanthracene(CA) by bromide anions are dependent on the size of the redoxinert ('innocent') tetraalkylammonium countercations in the low polar solvent dichloromethane, but not in well solvating media as acetonitrile or acetonitrile/water 1 : 1 (v : v).

In common electron transfer theory, only the interactions between isolated donor and acceptor molecules and solvent molecules are considered. This is sufficient, if the reactants are neutral and/or the reaction takes place in good solvation media (Fig. 1a). However, if electron transfer reactions between charged reactants are investigated in badly solvating media, the corresponding counterions become a part of the precursor, and successor complexes, respectively. In this case, multipolar interactions between reactant ions and counterions occur. This is illustrated in Fig. 1b. In the case of isolated donor and acceptor molecules, the precursor structure is sufficiently described by the distance between the reactants. There are no orientational effects. But if ion pairing is important, the microscopic electron transfer rates should depend on the mutual orientation of the reactants and the counterion. This is illustrated schematically in Fig. 1c. In addition to the donor-acceptor distance, also the relative position of the counterion determines the precursor structure. In the upper part of Fig. 1c the countercation is placed between the reactants. This leads to favourite coulomb interactions in both precursor and successor complexes. However, the overlap between the wave functions of donor and acceptor molecules is diminished due to the interference by the counterion. In the lower part of Fig. 1c, the donor and acceptor molecules are placed in contact, maximizing the overlap. However, in this extreme case, the electron is transferred away from the cation. This leads to a very unfavourable coulomb term. Therefore, the position of the countercation is quite important for the microscopic

* Corresponding author.

PII: S1010-6030(99)00214-2

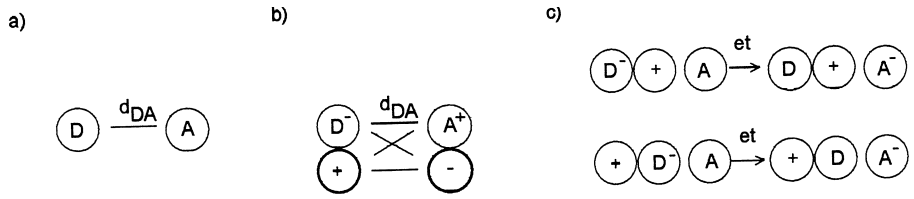

Fig. 1. Schematic description of electron transfer in the absence (a) and presence (b, c) of ion pairing, see text.

electron transfer rate constant. This holds also for our example of cyanoanthracenes and halides in dichloromethane.

Moreover, in fluid media the ions and molecules in the precursor complex fluctuate with respect to their mutual positions, and the electron transfer may occur from different distances with different probability. Fitting the parameters of the precursor structure to the electron transfer rate constants in this paper means therefore to estimate mean distance parameters between cyanoanthracene, halide and tetraalkyl ammonium cation during electron transfer.

Electronically excited cyanoanthracenes (^{1*}DCA/CA) are effectively quenched by an electron transfer mechanism [12] with a following fast thermal back reaction. Due to ion pair formation between halide anions (X^-) and the tetra-alkylammonium cations (TRA^+) in dichloromethane [13] the cations may influence the forward electron transfer rate. Applying the usual simplified kinetic scheme for electron transfer to our example, the relation between k_q and the diffusion rate constants k_{diff}, k_{-diff}, and the electron transfer rate constant k_{et} gives Eq. (1).

$$^{1*}\mathrm{DCA/CA} + \{\mathrm{TRA}^+, \mathrm{X}^-\} \underset{k_{-\mathrm{diff}}}{\overset{k_{\mathrm{diff}}}{\Leftrightarrow}}$$

$$[^{1*}\underset{\text{precursor complex}}{\mathrm{DCA/CA} + \{\mathrm{TRA}^+, \mathrm{X}^-\}}] \overset{k_{\mathrm{et}}}{\rightarrow}$$

$$[^{1*}\underset{\text{successor complex}}{\mathrm{DCA/CA}^{\cdot -}, \{\mathrm{TRA}^+, \mathrm{X}^{\cdot}\}}] \overset{k_{-\mathrm{et}}}{\rightarrow} \mathrm{DCA/CA}$$

$$+\{\mathrm{TRA}^+, \mathrm{X}^-\} \qquad k_q = \frac{k_{\mathrm{et}} k_{\mathrm{diff}}}{k_{\mathrm{et}} + k_{-\mathrm{diff}}} \tag{1}$$

As the anthracene acceptor molecules are neutral, we assumed the stability constant of the precursor complex to be

$$\frac{k_{\mathrm{diff}}}{k_{-\mathrm{diff}}} = \frac{4\pi N_{\mathrm{A}} d^3}{3} \tag{2}$$

with the Avogadro constant N_A and $d = r_A + r_D + r_K$, where r_A, r_D, r_K means the radius of the anthracene acceptor, halide donor and cation, respectively.

The electron transfer constants were determined as

$$k_{\mathrm{et}} = \frac{3}{4\pi N_{\mathrm{A}} d^3} \frac{1}{((1/k_q) - 1/k_{\mathrm{diff}})} \tag{3}$$

Taking into account that ion pairs exist between halide and cations, k_{diff} was calculated from Eq. (4).

$$k_{\mathrm{diff}} = \frac{2k_{\mathrm{B}} T N_{\mathrm{A}}}{3\eta} \left(2 + \frac{r_{\mathrm{A}}}{r_{\mathrm{D}} + r_{\mathrm{K}}} + \frac{r_{\mathrm{D}} + r_{\mathrm{K}}}{r_{\mathrm{A}}}\right) \tag{4}$$

The anthracene acceptor radii were approximated as ellipsoids with the semiaxis $a > b > c$ and $r_A \approx (a + b + c)/3$ [14]. $r_{A(DCA)} = 309$ pm, $r_{A(CA)} = 283$ pm derived from geometry optimized bond lengths of an AM1 calculation, the crystallographic radii $r_{D(Cl^-)} = 181$ pm, $r_{D(Br^-)} = 196$ pm, and viscosity $\eta = 0.43$ cP were used.

The electron transfer rate constants k_{et} decreased exponentially and more strongly than the quenching constants with increasing radius of the cations r_K and were fitted to the model Eq. (5)

$$k_{\mathrm{et,na}} = \frac{1}{1 + (4\pi V^2/\hbar\lambda)\tau_l} \frac{2\pi}{\hbar} \frac{1}{\sqrt{4\pi\lambda RT}} V^2 \times \exp\left(-\frac{(\Delta G_{\mathrm{et}} + \lambda)^2}{4\lambda RT}\right) \tag{5}$$

with the longitudinal relaxation time, $\tau_l = 0.4$ ps for dichloromethane, the electronic coupling matrix element V, the reorganization energy λ, the free energy of electron transfer $\Delta G_{et.}$ h means Planck constant , and k_B Boltzmann constant. The cation size has influence on the donor acceptor distance d_{DA} during electron transfer, on the solvent reorganization energy λ_S, the electronic coupling matrix element V, and the work term E_{work} in ΔG_{et}.

$$\lambda_{\mathrm{S}} = 14.41 \left(\frac{1}{2r_{\mathrm{A}}} + \frac{1}{2(r_{\mathrm{D}} + r_{\mathrm{K}})} - \frac{1}{d_{\mathrm{DA}}}\right)\left(\frac{1}{n^2} - \frac{1}{\varepsilon_{\mathrm{S}}}\right) \tag{6}$$

$n = 1.424$ is the refractive index and $\varepsilon_S = 8.93$ the relative dielectric permittivity.

The electronic coupling matrix element depends exponentially on the donor acceptor distance d_{DA} in the precursor complex, which is connected with the other geometric parameters, Figs. 2, Eq. (7)

$$d_{\mathrm{DA}} = \sqrt{(r_{\mathrm{D}} + r_{\mathrm{K}})^2 + d_{\mathrm{KA}}^2 - 2(r_{\mathrm{D}} + r_{\mathrm{K}}) d_{\mathrm{KA}} \cos(\alpha)} \tag{7}$$

$$V = V_0 \exp\left(-\left(\frac{\beta}{2}\right)(d_{\mathrm{DA}}) - (r_{\mathrm{D}} + r_{\mathrm{A}})\right) \tag{8}$$

Here V_0 is the electronic coupling matrix element at contact distance $(r_D + r_A)$, and β is a constant characteristic for the decay of electronic interaction with distance, see e.g. [15]. The free energy of the electron transfer between precursor and successor complexes ΔG_{et} could be estimated from the redox potentials of the donor halides $E^0(D^+/D)$ and acceptor anthracenes $E^0(A/A^-)$ as follows.

$$\Delta G_{\mathrm{et}} = E^0(\mathrm{D}^+/\mathrm{D}) - E^0(\mathrm{A}/\mathrm{A}^-) - E_{0\text{–}0} + E_{\mathrm{work}} \tag{9}$$

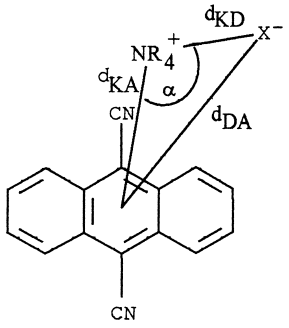

Fig. 2. Simplified model of the precursor structure, were d_{KA} is the distance between the tetra-*n*-alkylammonium cation and the acceptor, d_{KD} the distance between the tetra-*n*-alkylammonium cation and the donor, and α the angle between acceptor, cation and donor.

$E_{0–0}$ means the singlet excitation energy, and E_{work} the difference in coulomb stabilization energy between precursor and successor complex.

The work term E_{work} results essentially from the difference of coulomb stabilization of the ion pair in the precursor complex and the cation/reduced acceptor ion-pairs in the successor complex. It can be obtained by

$$E_{work} = \frac{14.41}{\varepsilon}\left(\frac{1}{r_D + r_K} - \frac{1}{d_{KA}}\right)[eV] \quad (10)$$

According to Fig. 2, d_{DA} is connected with d_{KA} by Eq. (7). d_{KA} and α as unknown geometric parameters and V_0 and β are the parameters to fit the k_{et} values according to Eq. (5). As the coulomb stabilization of the $NR_4^+X^-$ ion pairs is certainly much larger than any interaction with the neutral anthracenes, we assume that the donor cation distance $d_{KD} = r_D + r_K$ does not change.

With experimental data for cyanoanthracenes and bromide given in [11] and new experimental values of k_q for $^1DCA^* +$ chloride we carried out refined calculations by means of equations given above, in particular with redox potentials corrected for the solvent dichloromethane. As the radii of the cations seem to be important input parameters in order to calculate k_{et} from quenching constants k_q, we compared the results using cation radii calculated by molecular modelling as in [11], and using crystallographic radii [16]. We will show, that different consistent sets of cation radii give similar fitting parameters. Quantum chemical calculations of the electronic coupling matrix element *V* are compared with the values derived from electron transfer rate constants.

2. Procedures

2.1. Materials and fluorescence measurements

Chemicals and stationary fluorescence equipment were the same as described in [11], time resolved fluorescence data were obtained by means of a single photon counting apparatus (Edinburgh Instruments). k_q was derived from the slope of linear Stern–Volmer plots with at least five different quencher concentrations, error limits are standard deviations.

2.2. Calculations

As we could not find a complete set of experimentally determined radii of the tetra-alkylammonium cations in the literature, one set of cation radii was obtained by molecular modelling with the Cerius2 packet of Molecular Simulations. All-trans conformation of the alkyl chains was assumed and the radius was determined by averaging over the three space directions. For an estimation of the inner-sphere reorganization energy bond lengths and force constants of the excited anthracenes and anthracene radical anions were calculated by means of AM1 (Hyperchem for Windows, Hypercube.). As the inner-sphere reorganization energy proved to be negligible (≈0.01 eV), only the solvens reorganization energy λ_S was considered in the equations given above. The coefficients of the wave functions of reactants in Eq. (13) were calculated by means of PPP-SCF-CI calculations. Satisfying results can be expected with this method as in test calculations $E_{0–0} = 3.15$ eV for DCA was obtained in excellent agreement with the experimentally determined 3.12 eV from LIF spectra of jet-cooled DCA molecules [17]. The relevant $E_{0–0}$-value in dicloromethane is expected to be between the latter and the experimental value of 2.89 eV [18] in acetonitrile, which was used in our calculations.

3. Results and discussion

In Table 1 rate constants k_q of stationary and time resolved measurements are summarized. The time resolved data are less precise but in reasonable agreement with those of the stationary experiments. The electron transfer rate constants k_{et} were therefore calculated from the data of the stationary experiments by means of Eqs. (1)–(3), see Table 2.

In Fig. 3 the electron transfer rate constants k_{et} for quenching of ^{1*}DCA by Br^- and Cl^- are plotted against the cation radius. It is surprising that there is not much difference between the electron transfer rate constants (all within factor two for a specific cation) in quenching of ^{1*}DCA by Br^-, and Cl^-, respectively, as in quenching ^{1*}DCA or ^{1*}CA by Br^- [11]. In water containing solvent mixtures a difference of factor 8 was found as expected from the redox potential differences between ^{1*}DCA, and Br^- and Cl^-, respectively [20].

By means of Eq. (11) and $\varepsilon_S = 8.93$ and 35.7 for dichloromethane and acetonitrile, respectively, the redox potentials of anthracenes and halides in acetonitrile from the literature were corrected for the lower solvation energy in dichloromethane, Table 3. In Eq. (11), *z* is the number of electrons transferred, *e* the elementary charge, and *r* the ion radius.

Table 1
Fluorescence quenching constants $k_q/10^9\,dm^3\,mol^{-1}\,s^{-1}$ of ^{1*}DCA by bromide and chloride in dichloromethane

Counterion	Br^-		Cl^-
	Stationary [3]	Time resolved	Stationary
$N^+(C_2H_5)_4$	7.54 ± 0.08	7.5 ± 0.3	5.77 ± 0.16
$N^+(C_3H_7)_4$	7.29 ± 0.09	6.6 ± 0.3	
$N^+(C_4H_9)_4$	6.60 ± 0.09	6.1 ± 0.3	4.88 ± 0.23
$N^+(C_5H_{11})_4$	6.67 ± 0.03	5.9 ± 0.3	
$N^+(C_6H_{13})_4$	6.26 ± 0.12	5.8 ± 0.3	3.96 ± 0.10
$N^+(C_7H_{15})_4$	6.27 ± 0.07	5.6 ± 0.3	
$N^+(C_8H_{17})_4$	5.97 ± 0.13	5.8 ± 0.3	
$N^+(C_{16}H_{33})_4$	5.41 ± 0.17	5.3 ± 0.3	2.87 ± 0.37

Table 2
Electron transfer rate constants $k_{et}/10^9\,s^{-1}$ of ^{1*}DCA by bromide and chloride, and ^{1*}CA by bromide in dichloromethane[a]

Counterion[b]	r_K/pm		$k_{et}/10^9\,dm\,mol^{-1}\,s^{-1}$		
	$r_{K,cal}$	$r_{K,cryst}$	$^{1*}DCA + Br^-$	$^{1*}DCA + Cl^-$	$^{1*}CA + Br^-$
$N^+(C_2H_5)_4$	202	400	17.0	11.2	11.4
$N^+(C_3H_7)_4$	320	452	9.27		5.53
$N^+(C_4H_9)_4$	413	494	5.63	3.32	3.49
$N^+(C_5H_{11})_4$	480	529	4.52		2.75
$N^+(C_6H_{13})_4$	560	559	3.15	1.74	2.00
$N^+(C_7H_{15})_4$	640	588	2.49		1.54
$N^+(C_8H_{17})_4$	720		1.85		1.23
$N^+(C_{16}H_{33})_4$	900		1.03	0.49	0.76

[a] Calculated by means of $r_{K,cal}$,
[b] The crystallografic radii $r_{D,Br^-} = 196$ pm and $r_{D,Cl^-} = 181$ pm were used [19].

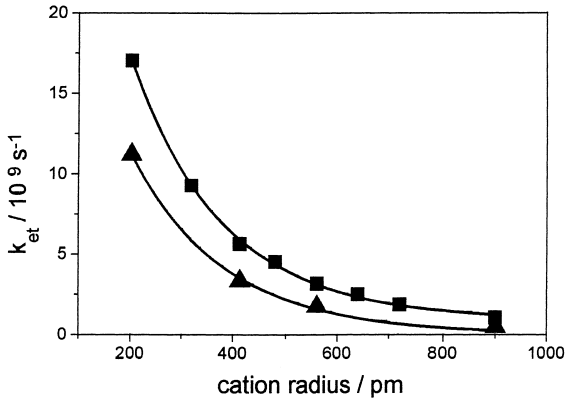

Fig. 3. Electron transfer rate constants k_{et} for quenching of ^{1*}DCA by Br^- (squares) and Cl^- (triangles) versus cation radii ($r_{K,cal}$, see text). Lines connect fitted values.

Table 3
Redox potentials in acetonitrile and dichloromethane[a]

Reactant	$E^0(D^+/D)$ (V)		$E^0(A/A^-)$ (V)	
	Acetonitrile	Dichloromethane	Acetonitrile	Dichloromethane
DCA			−0.98	−1.18
CA			−1.58	−1.80
Cl^-	1.86	1.52		
Br^-	1.47	1.16		

[a] Calculated according to Eq. (11) and the Faraday constant.

$$\Delta G_{solv} = -\frac{N_A z^2 e^2}{8\pi\varepsilon_0 r}(1 - 1/\varepsilon_S) \tag{11}$$

The four fit parameters of Eq. (5) given in Table 4 have to be considered as averages. They are compared for the two different sets of cation radii $r_{K,cal}$, and $r_{K,cryst}$, respectively. Between the third and fourth, and between the fifth and sixth column of Table 4, respectively, the differences of less than 20% show, that the absolute values of these radii are not critical for the results as far as consistent sets of data were used.

We estimate an uncertainty of 100% of the fit parameters due to the limited set of experimental data. Therefore, we restrict ourselves to two qualitative issues.

We consider the V_0-values of $<10\,cm^{-1}$ obtained as clear evidence for a nonadiabatic electron transfer.

The fitted cation-acceptor distance d_{KA} during the electron transfer is below the sum of $r_A + r_K$. The corresponding d_{KA}-values for electron transfer between $^1DCA^*$ and Br^- could be explained considering the smallest semiaxes of the anthracene and some penetration into the alkyl 'tentacles' of the cation. The d_{KA}-values calculated for the less exergonic electron transfer steps between $^1DCA^* + Cl^-$ and $^1CA^* + Br^-$ with less than 200 pm, however, are too low. If it is assumed that no screening by the solvent occurs, an increasing work term results applying Eq. (12) [21]. It would allow electron transfer from a something larger distance with d_{KA}-values which are given in the last three columns of Table 4.

$$E_{work} = \frac{14.41}{4}\left(\frac{1}{r_D + r_K} - \frac{1}{d_{KA}}\right) \tag{12}$$

Applying this latter calculation on the $^1DCA^* + Br^-$ case however results in d_{KA}-values which are too large.

According to Grampp and Jaenicke [14] the electronic coupling matrix element can approximately be determined by means of a HMO quantum chemical calculations according to Eq. (13).

$$V = \frac{\hbar^2}{m_e}\sum_r\sum_s \frac{c_{jr}c_{ks}}{d_{rs}}\left(\frac{\cos^2\xi}{\Delta^\sigma}S_0^\sigma \exp\left(-\frac{d_{rs} - d_0}{\Delta^\sigma}\right) - \frac{\sin^2\xi}{\Delta^\pi}S_0^\pi \exp\left(-\frac{d_{rs} - d_0}{\Delta^\pi}\right)\right) \tag{13}$$

Herein d_{rs}, m_e, c_{jr}, c_{ks}, is the mutual distance of atoms r and s, the mass of the electron, and are the coefficients of the wavefunctions of the reactants. The angle ξ determines the mutual orientation of donor anion and acceptor, see Fig. 4. S_0 and Δ are atom parameters of σ- and π-bonds, and d_0 is the van der Waals' distance of the atoms. The parameters Δ, S_0, and d_0 can be found in tables [22], except those for halides. Therefore, the data for oxygen were used, as calculations in that paper show, that parameters for different atoms do not vary much. Accordingly the same values for σ- and π-bonds were applied. c_{jr} -values were calculated by a PPP-SCF-CI method.

Table 4
Comparison of the fitting parameters for Eq. (5) using the two different sets of cation radii of Table 2[a]

	^{1*}DCA			^{1*}CA		^{1*}DCA	^{1*}CA	
	Cl^-	Br^-		Br^-		Cl^-	Br^-	
	$r_{K,cal}$	$r_{K,cal}$	$r_{K,cryst}$	$r_{K,cal}$	$r_{K'cryst}$	$r_{K,cal}$	$r_{K,cal}$	$r_{K,cryst}$
d_{KA}/pm	185	441	498	146	183	413	313	342
α/°	147	74	81	164	173	59	70	120
V_0/cm^{-1}	6.6	6.8	7.4	7.5	6.7	4.5	4.7	6.7
β/pm^{-1}	35	44	40	29	35	45	27	50

[a] Fitting of chloride values was performed with four rate constants determined experimentally and three interpolated values (linear interpolation with respect to rate constants and cation radii). Fit parameters in the last three columns were calculated using Eq. (12), see text.

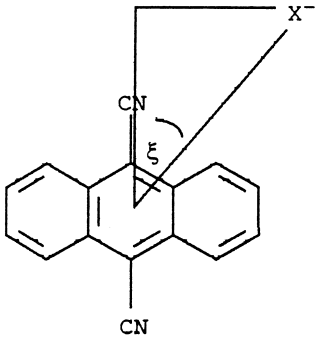

Fig. 4. Mutual orientation (angle ξ) of halide donor X^- in a plane with fixed distance of 3 Å from the ^{1*}DCA donor plane for calculations according to Eq. (13).

In calculations of V by means of Eq. (13) the donor position was stepwise changed in a plane with a fixed distance of 300 pm from the acceptor plane. The coupling matrix element values V calculated are shown as a contour map in Fig. 5. They cover 0–18 cm^{-1} depending on the orientation of donor and acceptor and reflect the molecular symmetry

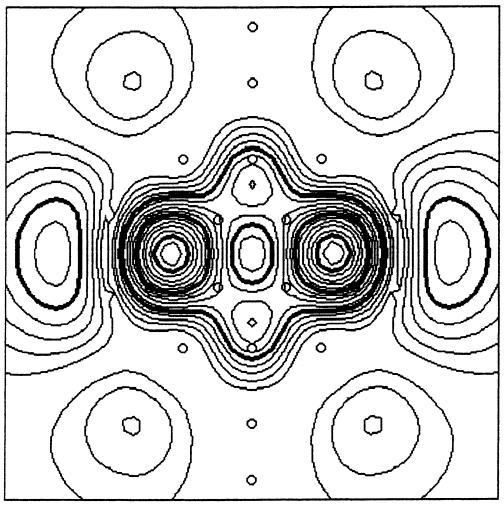

Fig. 5. Contour map of the calculated electronic coupling matrix elements V (cm^{-1}) for the electron transfer reaction $^{1*}DCA + Br^- \rightarrow DCA^{-\bullet} + Br^{\bullet}$ using geometry of Fig. 4 (axis scale 10 Å, contour line difference 1 cm^{-1}). As a gide for the eyes, strong contour lines for 5, 10, and 15 cm^{-1} (from outside to inside) are given.

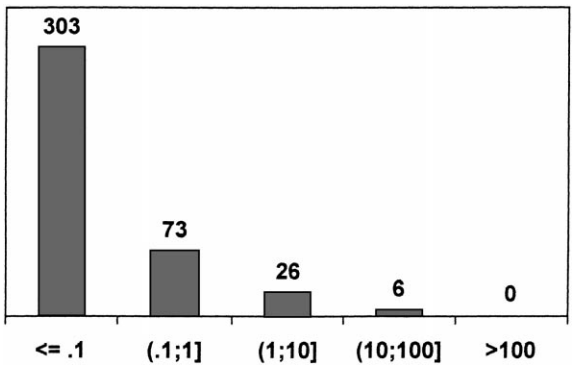

Fig. 6. Histogram of the calculated values of the electronic coupling matrix element V (cm^{-1}) for the electron transfer reaction $^{1*}DCA + Br^- \rightarrow DCA^{-\bullet} + Br^{\bullet}$. The data correspond to equidistant positions of the donor anion on a sphere surface at a fixed distance of 500 pm from the center of the acceptor molecule.

of DCA. These data illustrate, that contrary to the simplified assumptions of the model in Eq. (8), the value of the coupling matrix element is dependent on distance and orientation of donor and acceptor. Moreover the coupling matrix element was calculated for equidistant positions of the donor anion on a sphere surface around the center of the acceptor molecule in a distance of 500 pm. Molecular symmetry of DCA allows to restrict to a quarter of the sphere surface. The histogramm in Fig. 6 shows, that only about 6% of the 408 values of the coupling matrix element are in the range between 1 and 10 cm^{-1}, which are comparable to the mean value of V_0 derived from the fit to the experimental rate constants. The countercation could not be included in these quantum chemical calculations.

4. Summary

Rate constants of fluorescence quenching of cyanoanthracenes by chloride and bromide anions with a set of tetra-alkylammonium cations decrease with increasing alkyl chain length in dichloromethane. This is due to ion pair formation in dichloromethane and therefore varying ‘sterical hindrance’ by the redoxinert counterions of increasing size

in the electron transfer step. However the counterion may also act as a 'catalyst' in stabilizing the successor complex electrostatically. Electron transfer probability is highest in an optimal position with respect to donor, countercation and acceptor. The sphere symmetry of electron transfer probability is then no longer valid. Instead some 'microstructuring' of electron transfer probability governs the electron transfer rate. This may explain surprisingly high values of quenching by chloride with respect to the weak exergodicy of the electron transfer calculated without considering the countercation. Our model illustrates that the countercation may contribute to a more favourite energetics. Due to our experimental model system with a neutral molecule as an acceptor and a charged atom as a donor, simple quantum chemical calculations may support our neglection of the inner reorganization energy and the order of magnitude of the electronic coupling matrix element confirming nonadiabatic electron transfer. Our study shows that in low polar media the distance and orientation of redoxinert counterions with respect to donor and/or acceptor may finetune the rate of electron transfer steps. The idea of the influence of electrostatic interactions in electron transfer between proteins was currently discussed [23] and might generally be of importance in complex biological systems.

Acknowledgements

Financial support by Sächsisches Staatsministerium für Wissenschaft und Kunst and by Fonds der Chemischen Industrie ist gratefully acknowledged. T. K. thanks Studienstiftung des deutschen Volkes for a grant.

References

[1] P. Piotrowiak, J.R. Miller, J. Phys. Chem. 96 (1993) 7187.
[2] P. Piotrowiak, Inorg. Chim. Acta 225 (1994) 269.
[3] P. Piotroviak, Adv. Chem. Ser. (Photochemistry and Radiation Chemistry) 254 (1998) 219.
[4] P.D. Metelski, T.W. Swaddle, Inorg. Chem. 38 (1999) 301.
[5] L.-Z. Cai, D.M. Kneeland, A.D. Kirk, J. Phys. Chem. A 101 (1997) 3871.
[6] J. Coddington, S. Wherland, Inorg. Chem. 35 (1996) 4023.
[7] C.D. Clark, M.Z. Hoffman, J. Phys. Chem. 100 (1996) 7526.
[8] C.D. Clark, M.Z. Hoffman, J. Photochem. Photobiol. A 111 (1997) 9.
[9] C.D. Clark, M.Z. Hoffman, Coord. Chem. Rev. 159 (1997) 359.
[10] A. Marcus, J. Phys. Chem. B 102 (1998) 10071.
[11] T. Kluge, H. Knoll, O. Brede, Z. Physik. Chem. 191 (1995) 59.
[12] M. Mac, J. Wirz, Chem. Phys. Lett. 211 (1993) 20.
[13] L. Song, W.C. Trogler, J. Am. Chem. Soc. 114 (1992) 3355.
[14] G. Grampp, W. Jaenicke, Ber. Bunsenges. Phys. Chem. 95 (1991) 904.
[15] G. J. Kavarnos, Fundamentals Of Photoinduced Electron Transfer, VCH Publishers, New York, 1993, p. 308.
[16] P.K. Muhuri, D.K. Hazra, Z. Phys. Chem. 190 (1995) 111.
[17] S. Hirayama, F. Tanaka, Chem. Phys. Lett. 147 (1987) 447.
[18] J. Eriksen, C.S. Foote, J. Phys. Chem. 82 (1978) 2659.
[19] J.d′ Ans, E. Lax, Taschenbuch für Chemiker und Physiker 1992, Springer, Berlin.
[20] K.A. Abdullah, T.J. Kemp, J. Photochem. 28 (1985) 61.
[21] P. Suppan, J. Chem. Soc Faraday Trans. 1 82 (1986) 509.
[22] V.M. Bednikov, G.A. Bogdanchikov, Russ. J. Phys. Chem. 53 (1979) 155.
[23] Y. Feng, R.P. Swenson, Biochemistry 36 (1997) 13617.